Manipulation of Hyperbranched Polymers' Conformation

Michael E. Mackay*

Department of Chemical Engineering and Materials Science, Michigan State University, East Lansing, Michigan 48824

Glenda Carmezini

Department of Chemical, Biochemical and Materials Engineering, Stevens Institute of Technology, Castle Point on the Hudson, Hoboken, New Jersey 07030

Received July 23, 2001. Revised Manuscript Received November 16, 2001

The hydrodynamic volume for a series of hyperbranched polymers was studied to determine the volume change in a variety of solvents. The chemically different interior core and branching units were found to readily expand and contract by a factor of 2 creating large or small free volume, respectively. Furthermore, a solvent that maximally swells the polymer created a viscosimetric (hydrodynamic) radius which changed linearly with molecular mass. This is contrary to what is expected for dendrimers where the radius has been shown to scale with ln(M). A model was developed to account for the effect of molecular mass polydispersity on the intrinsic viscosity (viscosimetric volume), since hyperbranched polymers are polydisperse in nature, and it was found that this did not affect the observation. Solvents that contracted the hyperbranched polymers showed a complicated hydrodynamic radius scaling with mass. It was generally concluded that these polymers readily change volume with solvent effects important in influencing the change. Further results with a similar hyperbranched polymer having alkane rather than hydrogen end groups revealed a polymer that did not swell or contract as much (10% variation) for a wide range of solvents. In addition, this polymer had lower overall free volume and was found to behave in a manner that was quite similar to sterically stabilized particles. Thus, the core−shell molecular morphology, as well as its utility, depends quite strongly on the end groups and rational design of hyperbranched molecules must consider thermodynamic interactions with the solvent and within the molecule itself.

Introduction

Dendrimers, like hyperbranched polymers, are highly branched polymers with the first structure drawn probably over 50 years ago[1] (see Figure 2b). Reported research has grown significantly over the past decade, and several groups have published work describing synthesis and applications for dendrimers.[2−7] A key property of dendrimers is their molecular architecture which allows a core−shell morphology to be manipulated with the ability to sequester guest molecules.[8,9] The shell (dendrimer end groups) provides a solubilizing

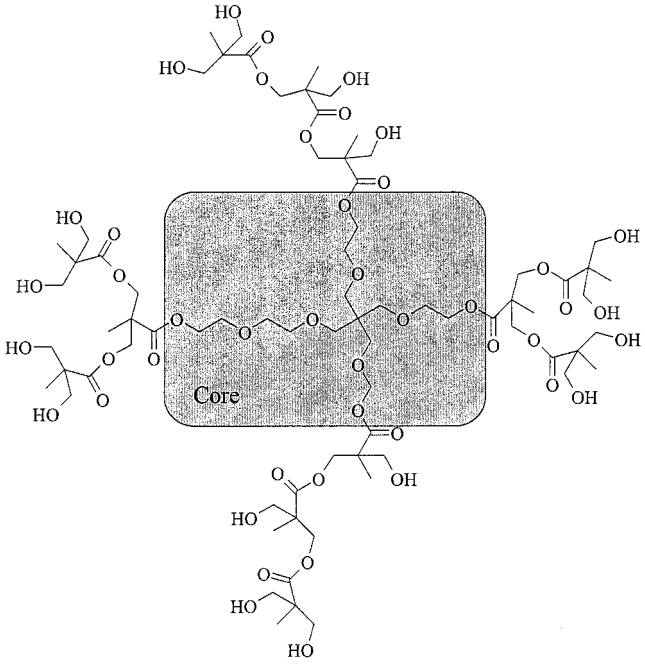

Figure 1. Schematic representation of an H20 molecule based on stoichiometry. The molecular core is indicated in the figure and is surrounded by the branching units with hydrogen end groups.

* To whom correspondence should be addressed. E-mail: mackay@msu.edu. URL: www.dendrimer.org.

(1) Zimm, B. H.; Stockmayer, W. H. *J. Chem. Phys.* **1949**, *17*, 1301−1314.
(2) Hawker, C. J.; Fréchet, J. M. J. *J. Am. Chem. Soc.* **1990**, *112*, 7638−7647.
(3) Fréchet, J. M. J. *Science* **1994**, *263*, 1710−1715.
(4) Tomalia, D. A. *Sci. Am.* **1995**, *May 1995*, 62−66.
(5) Tomalia, D. A.; Naylor, A. M.; Goddard, W. A. *Angew. Chem., Int. Ed. Engl.* **1990**, *29*, 138−175.
(6) Newkome, G. R.; Moorefield, C. N.; Vogtle, F. *Dendritic Molecules: Concepts, Syntheses, Perspectives*; John Wiley & Sons: New York, 1996.
(7) Bosman, A. W.; Janssen, H. M.; Meijer, E. W. *Chem. Rev.* **1999**, *99*, 1665−1688.
(8) Jansen, J. F. G. A.; Berg, E. M. M. d.-v. d.; Meijer, E. W. *Science* **1994**, *266*, 1266−1229.
(9) *Dendrimers III Design, Dimension, Function*; Vögtle, F., Ed.; Springer: New York, 2001; Vol. 212, p 198.

10.1021/cm010623r CCC: $22.00
Published on Web 01/23/2002

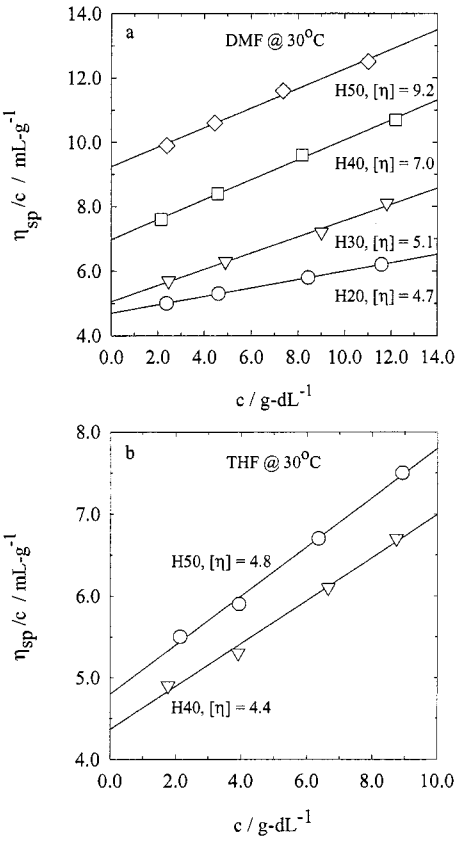

Figure 2. Specific viscosity divided by polymer concentration vs concentration for the H20−H50 series of hyperbranched polymers in (a) *n*,*n*-methyl-formamide (DMF) and (b) tetrahydrofuran (THF) at 30 °C. The plots are linear indicating that the intrinsic viscosity (intercept) and Huggins constant (slope) are not affected by polymer aggregation.

molecular attribute that may also be designed to target sites within a given application providing self-organization, drug delivery, and so forth, while the core can be chemically designed to interact with the guest molecule.

However, dendrimers are not completely rigid and different solvents can swell or contract the molecule[10] creating a physical interaction between the core and guest molecules. The work of Matos et al.[11] clearly demonstrated the dendrimer's ability to collapse through solvent change which in turn affected fluorescence decay of a centrally located porphyrin. Specifically, the flexibility of the core focal point was found to be a significant factor in dendrimer conformation.

In this work, the effects of solvent and end group type on the size of hyperbranched polymers (HBPs) or imperfect dendrimers is determined. While dendrimers certainly have a more regular structure than HBPs, potential applications are (probably) greater for HBPs due to their relatively simple synthesis.[12−18] The penalty for synthesis ease is polydispersity and propensity for cycle formation within the macromolecule.[19]

The core−shell attribute of HBPs was demonstrated through the work described by Muscat and van Benthem.[20] A stearate modified hyperbranched polyesteramide was found miscible with polypropylene. The shell (stearate alkane chain) provided miscibility while the polar core became susceptible to dyeing with conventional dyes, a difficult task to achieve with polypropylene. The cause of HBP miscibility with linear polymers is not fully understood at this time. Our work shows that linear low-density polyethylene and alkane-tipped HBPs (H3200)[21,22] are immiscible while stearate alkane chains seem to cause miscibility with polypropylene. Further work by us has shown that H3200 can be miscible with different architecture polyolefins;[23] thus, whether miscibility or phase separation occurs is dependent on, at this point, unknown thermodynamic interactions. However, the core−shell molecular morphology is a certain cause for the individual polymer−HBP thermodynamic interactions.

The effect of the core−shell molecular morphology on the molecule free volume and its distribution is considered in this work to gain further understanding of this unique molecular architecture. It is hoped that rational molecular design can then be made with the aim of predictive property creation like controlled phase separation, self-assembly, drug delivery, or chemical absorption as demonstrated through the dyeing of polypropylene fibers.

Experimental Section

Materials. The HBP used is an hydroxyl-functional dendritic polyester based on 2,2-bis-methylopropionic acid (bis-MPA) with an ethoxylated pentaerytriol (PP50) core[15,24] obtained from Perstorp Specialty Chemicals (Boltorn; Perstorp AB, Sweden). They are designated by H20, H30, and so forth as shown in Table 1 where, for example, H20 was manufactured with a stoichiometric ratio equal to a pseudo-second generation four-functional core dendrimer. An example of the structure for H20 is given in Figure 1. The core is taken as $C(CH_2OCH_2CH_2O-)_3(CH_2OCH_2CH_2OCH_2CH_2O-)$ with $-CO-CCH_3(CH_2O-)_2$ branching units and hydrogen (H) end groups. Note that the side branches to the left and right are drawn as perfect dendrimers while the upper and lower units are not.

The structure and extent of reaction for each generation HBP in this series has been questioned recently.[19] These researchers used vapor pressure osmometry to determine the number average molecular mass (M_n) as shown in the table. The theoretical molecular mass is also given (M_t), and a large deviation is seen. The approximate number of branching units

(10) Jeong, M.; Mackay, M. E.; Hawker, C. J.; Vestberg, R. *Macromolecules* **2001**, *34*, 4927−4936.
(11) Matos, M. S.; Hofkens, J.; Verheijen, W.; deSchryver, F. C.; Hecht, S.; Pollack, K. W.; Fréchet, J. M. J.; Forier, B.; Dehaen, W. *Macromolecules* **2000**, *33*, 2967−2973.
(12) Wooley, K. L.; Hawker, C. J.; Fréchet, J. M. J. *J. Am. Chem. Soc.* **1991**, *113*, 4252−4261.
(13) Malmström, E.; Johansson, M.; Hult, A. *Macromolecules* **1995**, *28*, 1689−1703.
(14) Ihre, H.; Hult, A.; Soderlind, E. *J. Am. Chem. Soc.* **1996**, *118*, 6388−6395.
(15) Malmström, E.; Johansson, M.; Hult, A. *Macromol. Chem. Phys.* **1996**, *197*, 3199−3207.
(16) Emrick, T.; Chang, H.-T.; Fréchet, J. M. J. *J. Polym. Sci., Part A*: *Polym. Chem.* **2000**, *38*, 4850−4869.
(17) Lin, Q.; Long, T. E. *J. Polym. Sci., Part A*: *Polym. Chem.* **2000**, *38*, 3736−3741.
(18) Voit, B. *J. Polym. Sci., Part A*: *Polym. Chem.* **2000**, *38*, 2505−2525.
(19) Burgath, A.; Sunder, A.; Frey, H. *Macromol. Chem. Phys.* **2000**, *201*, 782−791.
(20) Muscat, D.; van Benthem, R. A. T. M. in ref. 9, 41−80.
(21) Hong, Y.; Cooper-White, J. J.; Mackay, M. E.; Hawker, C. J.; Malmström, E.; Rehnberg, N. *J. Rheol.* **1999**, *43*, 781−793.
(22) Hong, Y.; Coombs, S. J.; Cooper-White, J. J.; Mackay, M. E.; Hawker, C. J.; Malmström, E.; Rehnberg, N. *Polymer* **2000**, *41*, 7705−7713.
(23) Mackay, M. E.; Carmezini, G.; Malmström, E.; Englund, J. In preparation.
(24) Malmström, E.; Hult, A.; Gedde, U. W.; Liu, F.; Boyd, R. H. *Polymer* **1997**, *38*, 4873−4879.

Table 1. Polymer Abbreviations Together with Their Molecular Masses[a]

polymer	M_n[b] (Da)	$[M - M_c]/M_0$	V_W (nm^3)	$[\eta]_W$ (mL g^{-1})
H20	827	4.1	0.667	1.21
H30	1320	8.4	1.049	1.20
H40	1730	12.0	1.366	1.19
H50	1970	14.0	1.552	1.19
H3200	4600		4.976	1.64
polymer	M_t (Da)	$[M - M_c]/M_0$	V_W (nm^3)	$[\eta]_W$ (mL g^{-1})
H20	1747	12.1	1.379	1.19
H30	3604	28.3	2.816	1.18
H40	7316	60.6	5.689	1.17
H50	14 740	125.1	11.43	1.17
H3200	12 000		13.10	1.63

[a] The upper part of the table is based on the number average molecular mass (M_n) determined with vapor pressure osmometry[19] while the lower part is based on the theoretical molecular mass (M_t). The third column shows the molecular mass with the core mass subtracted ($M_c = 352$ Da) and divided by the branching units' mass ($M_0 = 115$Da) and so represents the approximate number of branching units. The fourth column is the van der Waals volume (V_W) based on the number of branching units, and the core with the fifth column shows the intrinsic viscosity of an equivalent sphere with a density based on V_W. [b] Molecular mass determined by vapor pressure osmometry (data of Burgarth et al.[19]).

was determined by subtracting the core molecular mass ($M_c = 352$ Da) from the total mass (M_n or M_t) and dividing by the branching unit's mass ($M_0 = 115$ Da).

The abbreviation H3200 is used to designate Boltorn H30 whose end groups were partially functionalized (~90%) with a mixture of eicosanoic and docosanoic acid leading to $C_{20/22}$ alkane chains as end groups. The synthesis was performed by Perstorp AB. The molecular masses given in the table are M_n for H30, with the molecular mass for 11 "C_{21}" alkanes added to cover ~90% of the terminal hydroxyl groups or M_t to cover ~29 terminal end groups.

Intrinsic Viscosity. The materials were prepared by a careful procedure. The H20−H50 series is fairly hygroscopic, and the samples that were received tended to have bound water. In fact, room temperature isopiestic measurements with H30 and H3200 showed that the equilibrium moisture content with saturated NaCl solutions was approximately 6.5 and 0.35 wt %, respectively. To prepare solutions for intrinsic viscosity measurements, the H20−H50 series was heated to ~120 °C in a beaker for 10 min and cooled to 50−60 °C and solvent was added. The solutions were allowed to homogenize at room temperature for at least 1 day, passed through 1.0 μm PTFE filters, and transferred to the Ubbelohde viscometer (size 1 or OC depending on the solvent flow time) contained in a constant-temperature bath (30 ± 0.01 °C).

The heating of the H20−H50 series of polymers was necessary, and it was noticed that water was released that otherwise would not readily occur under vacuum-drying at room temperature. This procedure also affected the intrinsic viscosity ($[\eta]$) values (more consistent values were obtained after heating) and simultaneously changed the solubility in the solvent used: toluene (Tol, solubility parameter = 8.9 (cal/cm^3)$^{1/2}$), tetrahydrofuran (THF, 9.1 (cal/cm^3)$^{1/2}$), benzene (Ben, 9.2 (cal/cm^3)$^{1/2}$), chloroform (Chl, 9.3 (cal/cm^3)$^{1/2}$), dichloromethane (DCM, 9.7 (cal/cm^3)$^{1/2}$), 1-methyl-2-pyrrolidinone (NMP, 11.3 (cal/cm^3)$^{1/2}$), and *n*,*n*-methyl-formamide (DMF, 16.1 (cal/cm^3)$^{1/2}$). Only after the heating procedure were H40 and H50 soluble in THF while H20 and H30 were only slightly soluble. The intrinsic viscosity was not measured for H20 and H30 in THF as the slight solubility interfered with obtaining consistent values. The properties of the H3200 samples were not as sensitive to the solutions' preparation procedure although a similar procedure to the H20−H50 series was followed.

Polymer solution concentrations (c) were measured as mass of polymer/volume of solution through evaporative drying. Utilization of mass of polymer/volume of solvent affected the intrinsic viscosity (and particularly the Huggins coefficient, k_H) values obtained through

$$\eta_{sp}/c = [\eta] + k_H[\eta]^2 c \quad (1)$$

so all data reported here were determined by knowing mass of polymer/volume of solution. The specific viscosity (η_{sp}) was found through the ratio of solution density (ρ) times solution flow time (t) divided by solvent density (ρ_0) and solvent flow time (t_0) via

$$\eta_{sp} = [\rho t/\rho_0 t_0] - 1$$

Solution densities were found with the use of a density bottle equilibrated to 30 ± 0.01 °C.

Example data plotted in the form of eq 1 are given in Figure 2. The data follow a linear trend indicating that only two molecule interactions are important (c^2 term) and polymer aggregation is not occurring. Importantly, if aggregation is present, the plots in Figure 2 tend to be upwardly curved; there is no evidence of this particularly for the marginally soluble H40 and H50 in THF.

Results and Discussion

Intrinsic Viscosity. The intrinsic viscosity ($[\eta]$) was determined for the H20−H50 and H3200 series of HBPs in a variety of solvents with results given in Table 2. Our results for H20−H50 in NMP are different from those obtained by Nunez et al.[25] These researchers prepared solutions by slowly dissolving the HBP in NMP and then diluting the solutions to find $[\eta]$. Our procedure involved heating of the neat HBP to release bound water, as outlined above, and we have determined that $[\eta]$ is larger by a factor of approximately 2 if our procedure is followed. Nunez et al. also found that $[\eta]$ for H30 was larger than $[\eta]$ for H40; we see no such behavior with $[\eta]$ smoothly increasing with molecular mass as shown in Figure 3a. The results presented here are believed to be a true representation of $[\eta]$ and are not influenced by bound water. See the appendix for further discussion.

The intrinsic viscosity for dendrimers is unique and exhibits a maximum at a certain generation or molecular mass. This phenomenon influences the molecular free volume and its distribution which can be delineated by a simple model. Mourey et al.[26] advanced a model where it was suggested that each reacted "layer" or generation ($g = 1, 2, ...$) on the dendrimer contributes linearly to the viscosimetric radius ($R_\eta \sim g$). Realizing that the molecular mass (M) for dendrimers scales as 2^g, one can arrive at the intrinsic viscosity scaling as $g^3/2^g$. (N.B. Einstein's viscosity relation gives $[\eta] = 5/2 \times V_\eta/M$, $V_\eta = 4/3 \times \pi R_\eta^3$. The factor of "2" in the molecular mass scaling comes from the assumed dendrimer functionality; the HBPs used here have a branching functionality of 2 as shown in Figure 1.) This simple model shows a maximum in $[\eta]$ with molecular mass at fourth generation. The maximum does not indicate a sudden collapse of the molecule since the volume is always increasing, rather, the molecular mass ultimately increases faster than the viscosimetric volume (V_η).

(25) Nunez, C. M.; Chiou, B.-S.; Andrady, A. L.; Khan, S. A. *Macromolecules* **2000**, *33*, 1720−1726.
(26) Mourey, T. H.; Turner, S. R.; Rubenstein, M.; Frechet, J. M. J.; Hawker, C. J.; Wooley, K. L. *Macromolecules* **1992**, *25*, 2401−2406.

Table 2. The Upper Half of the Table Shows the Polymer, Number Average Molecular Mass (M_n),[19] and Intrinsic Viscosity ([η]) in Three Different Solvents: THF, NMP, and DMF[a]; the Lower Part of the Table Shows the Intrinsic Viscosity for the H30 Polymer Having C_{20-22} Alkane End Groups (H3200) in Various Solvents[b]

polymer	M_n (Da)	THF (9.1) [η] (mL g^{-1})	NMP (11.3) [η] (mL g^{-1})	DMF (16.1) [η] (mL g^{-1})	THF (9.1) R_h (nm)	NMP (11.3) R_h (nm)	DMF (16.1) R_h (nm)
H20	827		6.9 (0.690)	4.7 (0.391)		0.97	0.85
H30	1320	3.7[c] (0.241)	7.6 (0.776)	5.1 (0.448)	0.92[c]	1.17	1.02
H40	1730	4.4 (0.347)	9.1 (0.868)	7.0 (0.703)	1.07	1.36	1.24
H50	1970	4.8 (0.405)	10.2 (0.882)	9.2 (0.870)	1.15	1.47	1.42

polymer	M_n (Da)	Tol (8.9) [η] (mL g^{-1})	THF (9.1) [η] (mL g^{-1})	Ben (9.2) [η] (mL g^{-1})	Chl (9.3) [η] (mL g^{-1})	DCM (9.7) [η] (mL g^{-1})
H3200	4600	5.6 (0.303)	5.8 (0.325)	5.8 (0.325)	6.3 (0.378)	6.1 (0.357)

polymer	M_n (Da)	R_h (nm)	R_h (nm)	R_h (nm)	R_h (nm)	R_h (nm)
H3200	4600	1.59	1.61	1.61	1.66	1.64

polymer	M_n (Da)	δ (nm)	δ (nm)	δ (nm)	δ (nm)	δ (nm)
H3200	4600	0.68	0.70	0.70	0.74	0.72

[a] The numbers given in parentheses underneath the solvent names are the solubility parameters for the solvents ((cal/cm^3)$^{1/2}$). The numbers in parentheses next to intrinsic viscosity values are the fractional free volumes calculated as described in the text. The last three columns show the hydrodynamic radius (R_h) also calculated as described in the text. The [η] value for H30 in THF was determined by fitting the H40 and H50 [η] values to a power law with molecular mass. [b] The R_h was calculated for this polymer and shown in the following row, and the final row gives the alkane hydrodynamic thickness (δ) as described in the text. [c] Extrapolated values obtained by using a power law of 0.67 for [η] with M, [η] $\sim M^{0.67}$. The power law is based on data for H40 and H50 in THF.

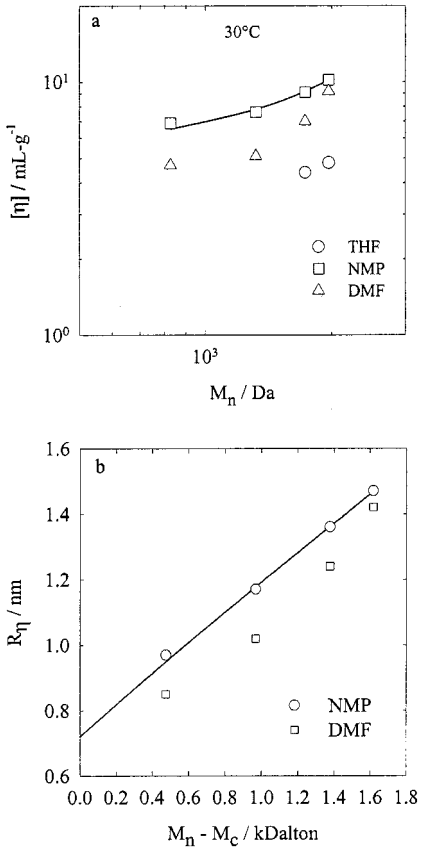

Figure 3. (a) Intrinsic viscosity vs number average molecular mass for the H20−H50 hyperbranched polymer series in tetrahydrofuran (THF), 1-methyl-2-pyrrolidinone (NMP), and *n*,*n*-methyl-formamide (DMF) at 30 °C. The solid line represents a fit to the data for the linear radius model given in eq 4b for NMP solvent. (b) Viscosimetric radius vs molecular mass of the branching units in NMP and DMF. The line is a fit of eq 4b to the data in NMP solvent.

This property of dendrimers is interesting and suggests that each dendrimer layer or generation is "pushed" or "pulled" toward the molecular perimeter. Thus, the segment (atom) density will be quite large at the perimeter. This may not be completely true, and Mansfield[27] has shown simulations where an intrinsic viscosity maximum with generation number is seen; however, significant segment back-folding is present, particularly for the outer layers, while the inner layers tend to be localized within certain regions. So, a mixture of layer-by-layer addition to the molecular radius and outer layer back-folding tends to yield a molecule with an intrinsic viscosity maximum and an approximately constant segment (atom) density across the molecular diameter.

The HBPs used here do not show a maximum of [η] with molecular mass as seen in Figure 3a; others have seen similar behavior.[28] It is readily discerned that [η] changes with the solvent for the H20−H50 series of polymers as well as for H3200 (see Table 2 and Figure 3a). Thus, the HBPs are flexible and can change volume by a factor of 2 in some cases. Jeong et al.[10] found similar behavior with poly(benzyl ether) dendrimers, and in one solvent, a molecular mass independent [η] was found indicating behavior like a constant density particle rather than a polymer.

The discussion below is aimed at determining the segment density or, conversely, the free volume within the HBP. A major motivation for HBP utilization is their core−shell molecular morphology that is capable of harboring guests.[29] For this to occur, the free volume must be large enough and perhaps distributed in a manner to accept the guests. We have used [η] as a convenient and accurate measure of molecular volume as well as a means to calculate free volume. Volumes determined by other techniques are amenable to similar interpretation.[30]

(27) Mansfield, M. *Macromolecules* **2000**, *33*, 8043−8049.
(28) Bodnar, I.; Silva, A. S.; Deitcher, R. W.; Weisman, N. E.; Kim, Y. H.; Wagner, N. J. *J. Polym. Sci., Part B: Polym. Phys.* **2000**, *38*, 857−873.
(29) Schmaljohann, D.; Potachke, P.; Hassler, R.; Voit, B. I.; Froehling, P. E.; Mostert, B.; Loontjens, J. A. *Macromolecules* **1999**, *32*, 6333−6339.

Free Volume. The volume change experienced in different solvents will affect the molecular free volume. To quantify this, the volume increments suggested by Edward[31] are used to determine the van der Waals volumes (V_W), given in Table 1, which are the minimum volumes that molecules can achieve. These were converted into $[\eta]$ values via the Einstein relation[32] to find the smallest value that can be attained by $[\eta]$, namely, $[\eta]_W$

$$[\eta]_W = 5/2 \times V_\eta/M = 5/2 \times V_W/M \quad (2)$$

also shown in Table 1. This intrinsic viscosity is approximately independent of the number average molecular mass as well as the theoretical molecular mass used (M_n or M_t), and the values of 1.2 mL/g (H20−H50) or 1.64 mL/g (H3200)are assumed in all calculations. Note that these values of $[\eta]_W$ are for a sphere with no free volume.

The fractional free volume ($f = V_f/V$; V_f is the free volume and V is the total volume) is calculated in the manner suggested by Hirschfelder, Eyring, and coworkers[33,34] for condensed matter

$$f = 8[1 - \{V_W/V\}^{1/3}]^3 = 8[1 - \{[\eta]_W/[\eta]\}^{1/3}]^3 \quad (3a)$$

or for gaslike states

$$f = 1 - V_W/V = 1 - [\eta]_W/[\eta] \quad (3b)$$

with the factor of 8 included in eq 3a by convention (with some theoretical justification). We take the minimum value of f from either eq 3a or 3b as representative of the molecular fractional free volume.

It is clear that the fractional free volume in H3200, alkane terminated HBP, is large, although it is not as large as an equivalent molecular mass HBP without the alkane end groups (see Table 2). This may be a reflection of the core−shell molecular morphology and the chemical dissimilarity of the alkane groups to the branching units and core. Group contribution techniques were used to determine the solubility parameters[35] for the core (9.9 $(cal/cm^3)^{1/2}$), branching unit (11.8 $(cal/cm^3)^{1/2}$), and alkane end groups (8.0 $(cal/cm^3)^{1/2}$) to reinforce this statement. Interestingly, the free volume for H3200 does not change by a large amount with a change in solvent. Poly(benzyl ether) dendrimers vary by a factor of 2 over the same solubility parameter range.[10]

The long chain alkanes serve as solubilizing agents for the HBP, thereby allowing clear solutions to be made in a range of solvents with a solubility parameter from 8.9 to 9.7 $(cal/cm^3)^{1/2}$. However, the alkanes do not seem to "expand" the core to create an interior with large free volume. To determine the distribution of free volume within H3200, the viscosimetric radius, R_η, for H30 in THF is calculated via (see eq 2, Flory[32] and Tande et al.[36] for a discussion of various molecular radii)

$$R_\eta = \{3/10\pi \times [\eta]M_n\}^{1/3}$$

by extrapolating $[\eta]$ in a power law with M_n for H40 and H50 to arrive at a value of 0.92 nm (see Table 2). This is taken as the "core" radius for H3200 and is subtracted from the viscosimetric radius for H3200 in the various solvents used here to arrive at a value of 0.71 ± 0.02 nm. (N.B. The core for H3200 is taken as the four-functional core and branching units (see Figure 1), while the alkane end groups are the shell.) This is similar in principle to the determination of hydrodynamic chain lengths (δ) for sterically stabilized particles.[37] The extended contour length for a C_{21} alkane is approximately 3 nm; thus, the alkane chains are extended into the solvent but not fully, at least in terms of hydrodynamics. Extrapolation of $[\eta]$ can be criticized, and if an average value for the H40 and H50 data is used (4.6 mL/g), R_η is found to be 0.99 nm for the core and δ is 0.78 ± 0.02 nm.

Further criticism can be leveled at either estimate of the core R_η by noting that H30 has terminal hydroxyl groups which could cause the collapse of H40 and H50 in THF. Since most of these hydroxyl groups (∼90%) are not present in H3200, calculation of the core R_η via this technique could be flawed. However, the hydrodynamic radius for a C_{21} alkane is ∼1.0 nm,[38] which is of the same order as our calculated δ value, and so we believe that this is consistent with our argument.

The free volume distribution can be found from the condensed matter expression (eq 3a) and the van der Waals volume for a single C_{21} alkane chain which is 0.357 nm^3. The volume for the alkane shell is 14.9 nm^3 ($4\pi/3 \times (1.63^3 - 0.92^3)$ nm^3), yielding a fractional free volume of 0.37 assuming that 11 alkane chains are attached to the pseudo-third generation HBP. This can be compared to the fractional free volume of H30 in THF, 0.24. Thus, the H3200 HBP has a dense central region ($f \sim 0.24$) surrounded by a less dense shell of alkane groups ($f \sim 0.37$). Furthermore, this density distribution does not seem to change with solvent which may be useful in some applications.

The situation is different for the H20−H50 series of HBPs as it shows a considerable volume change in different solvents. This is clearly seen in Figure 4, where the intrinsic viscosity divided by that at the maximum ($[\eta]_{max}$) is plotted vs the solvent solubility parameter. For a given polymer molecular mass, this type of plot is equivalent to the ratio of molecular volumes (see eq 2), and the solvent solubility parameter where the volume ($[\eta]$) exhibits a maximum is taken as the polymer solubility parameter.[10,39] Figure 4 is merely used to demonstrate the relative volume change since the occurrence of hydrogen bonding, which is surely present with the H20−H50 series dissolved in this range of solvents, and limits applicability of the solubility

(30) Burchard, W. *Adv. Polym. Sci.* **1999**, *143*, 113−195.
(31) Edward, J. T. *J. Chem. Educ.* **1970**, *47*, 261−270.
(32) Flory, P. J. *Principles of Polymer Chemistry*; Cornell University Press: Ithaca, 1953.
(33) Hirschfelder, J.; Stevenson, D.; Eyring, H. *J. Chem. Phys.* **1937**, *5*, 896−912.
(34) Glasstone, S.; Laidler, K. J.; Eyring, H. *The Theory of Rate Processes*; McGraw-Hill Book Co.: New York, 1941.
(35) Painter, P. C.; Coleman, M. M. *Fundamentals of Polymer Science*; Technomic Publishing: Lancaster, 1997.
(36) Tande, B. M.; Wagner, N. J.; Mackay, M. E.; Hawker, C. J.; Vestberg, R.; Jeong, M. *Macromolecules* **2001**, *34*, 8580−8585.
(37) Mewis, J.; Frith, W. J.; Strivens, T. A.; Russel, W. B. *AIChE J.* **1989**, *35*, 415−422.
(38) *Polymer Handbook*, 3rd ed.; Brandrup, J., Immergut, E. H., Eds.; John Wiley & Sons: New York, 1989. The relation $[\eta]$ (mL/g) = −1.14 + 0.104 M(Da) for $\sim C_{16}-C_{32}$ alkanes in carbon tetrachloride at 20 °C is given in this reference.
(39) Sheehan, C. J.; Bisio, A. L. *Rubber Chem. Technol.* **1966**, *39*, 149−192.

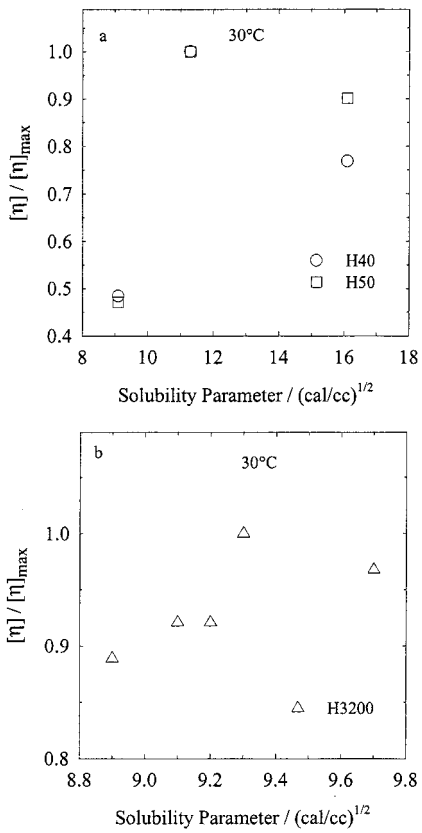

Figure 4. Intrinsic viscosity divided by that at the maximum vs solvent solubility parameter at 30 °C: (a) H40 and H50 and (b) H3200.

parameter as a quantitative measure of polymer−solvent interactions.[35]

Interpretation of the results for H3200 revealed a dense central region that is made of the core and branching units and is surrounded by a less dense shell of alkane end groups. Interpretation of the H20−H50 series is more involved. A simple model is assumed to account for the change in the viscosimetric volume with molecular mass to yield

$$[\eta] = 10\pi/3 \times \{R_c + K[M - M_c]\}^3/M \equiv 10\pi/3 \times R_\eta^3/M \quad (4a)$$

for the intrinsic viscosity where R_c is the core radius of molecular mass M_c (352 Da). This simple linear model suggests that a plot of viscosimetric radius as a function of molecular mass should yield a linear plot, which is indeed the case for H20−H50 in NMP (see Figure 3b). However, these HBPs are polydisperse in molecular mass[19] and eq 4a may not be strictly valid. In the Appendix, the Schulz−Flory molecular mass distribution was applied to eq 4a to arrive at the average intrinsic viscosity

$$\langle[\eta]\rangle = [\eta]_{M_n} + 10\pi/3 \times \{[R_c - KM_c]^3[\exp(M_c/M_n)E_1(M_c/M_n) - 1] + 3K^2M_nM_c[R_c - KM_c] + K^3M_n[M_n + M_c]^2\}/M_n \quad (4b)$$

where $[\eta]_{M_n}$ is the intrinsic viscosity calculated with M_n substituted in eq 4a and $E_1(\bullet)$ is the first exponential integral. Utilizing eq 4b to fit R_η data, one finds an essentially linear relation in NMP solvent, suggesting that the nonlinear terms in the curly brackets do not greatly contribute, as seen in Figure 3b. Values for R_c and K are 0.74 ± 0.02 nm and (3.64 ± 0.14) × 10^{-4} nm/Da, respectively. These parameters were used to predict the intrinsic viscosity, and as shown in Figure 3a, the prediction is quite adequate for the HBPs in NMP solvent.

The extended chain length for an arm of the four-functional core is approximately 0.9 nm (compared to $R_c = 0.74$ nm), and so the core arms are fairly extended making the fractional free volume quite large and equal to 0.68 ($V_w = 0.299$ and $V_\eta = 1.70$ nm^3). However, f is larger for the branching units. Using the fit results from eq 4b, one finds that f varies from approximately 0.7 (H20) to 0.9 (H50), indicating a fairly open structure for the branch units in NMP solvent. These free volumes are much larger than that for the H3200 molecule, and thus a more open structure exists.

Interpretation of the results in DMF solvent are more complicated; a linear relation is not seen for the viscosimetric radius with mass (see Figure 3b), and therefore interpretation becomes complicated due to the mass polydispersity. More involved models than that shown in eq 4a were developed, such as that expected for a dendrimer:[26] $R_\eta = C_1 + C_2 \ln(M - M_c)$, where C_1 and C_2 are constants. Yet, this model did not describe the data well. Generally, it does appear that the core and branching units are more densely packed in this solvent, DMF, as well as in THF.

Finally, it is possible that the molecular mass for H50 is slightly larger as discussed in the Appendix. If this is true, it is shown that the linear model given in eq 4a is applicable to both NMP and DMF solvents. Further work is needed to determine whether this observation is true, and merely note the possibility.

Conclusion

Hyperbranched polymers were shown to readily change volume in some cases. The neat HBPs used here (H20−H50 series) have a volume variation of approximately 2 with solvent change. This produced cores with a free volume of approximately 0.95 nm^3 that are capable of hosting a molecule with a radius of 0.61 nm. The free volume in the branching units was even larger, and therefore ready access to the chemically dissimilar interior core is possible. Solvent change may indeed allow trapping of the guest molecule within the core, and so a robust composite molecule may be possible. Furthermore, it may be possible to deliver the guest when the solvent is changed, or some other solvency condition is initiated, through the volume change.

The HBP with alkane end groups, H3200, was found to change volume to a lesser extent, and only a 10% variation is seen. This polymer was more similar to a sterically stabilized particle and had an interior free volume of the order of 1 nm^3 surrounded by the alkane chains. The interior volume does not change with solvency conditions, and therefore this HBP may be more amenable to applications where this characteristic is useful. Indeed this may be a key property that allows the dyeing of polypropylene fibers.[20]

Rational molecular design of HBPs for applications is needed. In this work, we have shown that chemical

Table A1. Comparison of Intrinsic Viscosity Data (in mL g^{-1} at 30 °C) from This Study and Others[a]

polymer	[η]-DMF this study	[η]-DMF Burgath et al.	percentage difference	[η]-NMP this study	[η]-NMP Nunez et al.	percentage difference
H20	4.7	4.3	−8.5	6.9	2.7	−61
H30	5.1	5.6	+9.8	7.6	3.8	−50
H40	7.0	6.8	−2.9	9.1	3.6	−60
H50	9.2	7.0	−24	10.2	4.2	−59

[a] The results from Burgath et al.[19] were gathered at room temperature while those from Nunez et al.[25] were probably determined at room temperature. The columns show the polymer, the present results in DMF, Burgath et al.'s results in DMF, percentage difference, the present results in NMP, Nunez et al.'s results in NMP, and percentage difference.

composition can have a significant effect on HBP volume change, which is surely a necessary condition for their utility.

Appendix

Intrinsic Viscosity Model. Here, eq 4a is corrected for polydispersity effects using the Schulz−Flory "most probable" molecular mass distribution.[40] Burgarth et al.[19] have stated that the molecular mass polydispersity index (PDI = weight to number average ratio) for the HBPs used here is approximately 2. We assume that the PDI is 2, as the most probable distribution inherently does; however, the mass distribution is taken as due to the variation of the branching units and the core is of constant mass to arrive at the following normalized distribution function

$$F(M)\,\mathrm{d}M = \{\exp(M_c/M_n)/M_n\} \times \exp(-M/M_n)\,\mathrm{d}M \qquad M_c \le M \le \infty$$

where F(M) dM represents the fraction of molecules with mass between M and (M + dM), M_c is the core mass and M_n, is the number average mass. Combining this with eq 4a yields the average intrinsic viscosity, $\langle[\eta]\rangle$

$$\langle[\eta]\rangle = \int_{M_c}^{\infty}[\eta]F(M)\,\mathrm{d}M = 10\pi/3 \times \{[R_c + K\{M_n - M_c\}]^3 + [R_c - KM_c]^3[\exp(M_c/M_n)E_1(M_c/M_n) - 1] + 3K^2M_nM_c[R_c - KM_c] + K^3M_n[M_n + M_c]^2\}/M_n$$

The first exponential integral, $E_1(\bullet)$, is given by[41]

$$E_1(z) = -\gamma - \ln(z) + z - z^2/4 + \cdots \qquad (9)$$

for small values of z; γ is Euler's constant and is equal to 0.57721....

(40) Peebles, L. H. *Molecular Weight Distributions in Polymers*; Interscience Publishers: New York, 1971.

(41) Abramowitz, M.; Stegun, I. A. *Handbook of Mathematical functions*; Abramowitz, M., Stegun, I. A., Eds.; Dover Publications: New York, 1972; p 1046.

Comparison of Intrinsic Viscosity Data. The sample preparation procedure described in this work was carefully followed to ensure elimination of bound water. This is known to influence the intrinsic viscosity and may possibly affect results gathered with other characterization techniques. A comparison of our intrinsic viscosity data with two other studies is given in Table A1. The difference is quite large between Nunez et al.'s[25] results and ours and, as discussed above, is probably the consequence of bound water. Comparison to the data of Burgath et al.[19] is more satisfactory although the largest molecular mass material, H50, may suffer bound water; note the negative deviation in the intrinsic viscosity. This sample may have been exposed to moisture following synthesis to have caused this deviation.

On the basis of the above observation, the molecular mass for H50 could quite possibly be larger and closer to the theoretical molecular mass, although we recognize that predicting the influence on a thermodynamic measurement such as vapor pressure osmometry is fraught with danger. Accepting that the molecular mass of H50 is 10% larger (2170 Da), for example, one can virtually eliminate curvature in the plot of R_η vs (M_n − M_c) shown in Figure 3b for DMF solvent. This is seen in the following linear least-squares fits to the data

DMF(M_n(H50) = 1970 Da):

$$R_\eta\,(\mathrm{nm}) = 0.588 + 4.93 \times 10^{-4}[M_n - M_c]\,(\mathrm{Da}) \quad R^2 = 0.975$$

DMF(M_n(H50) = 2170 Da):

$$R_\eta\,(\mathrm{nm}) = 0.606 + 4.66 \times 10^{-4}\,[M_n - M_c]\,(\mathrm{Da}) \quad R^2 = 0.990$$

The fits for data gathered in NMP solvent are not significantly affected, and the correlation coefficient (R^2) is unchanged and remains at 0.999 for both assumed H50 molecular masses (R_c changes a little: ∼3%). Thus, it is entirely possible that the molecular mass for H50 is larger and the linear radius model discussed above is applicable to both NMP and DMF solvents.

CM010623R